High Pressure Scanning Tunneling Microscopy Study of CO Poisoning of Ethylene Hydrogenation on Pt(111) and Rh(111) Single Crystals

David C. Tang,[†,‡] Kevin S. Hwang,[†,‡] Miquel Salmeron,[‡] and Gabor A. Somorjai*[,†,‡]

Department of Chemistry, University of California, Berkeley, California 94720 and Materials Sciences Division, Lawrence Berkeley National Laboratory, Berkeley, California 94720

Received: August 29, 2003; In Final Form: June 7, 2004

Using a high-pressure scanning tunneling microscope we monitored the coadsorption of hydrogen, ethylene, and carbon dioxide on platinum(111) and rhodium(111) crystal faces in the mtorr pressure range at 300 K in equilibrium with the gas phase. During the catalytic hydrogenation of ethylene to ethane in the absence of CO the metal surfaces are covered by an adsorbate layer that is very mobile on the time scale of STM imaging. We found that the addition of CO poisons the hydrogenation reaction and induces ordered structures on the single-crystal surfaces. Several ordered structures were observed upon CO addition to the surfaces precovered with hydrogen and ethylene: a rotated $(\sqrt{19} \times \sqrt{19})$R23.4° on Pt(111), and domains of c(4 × 2)-CO + C_2H_3, previously unobserved (4 × 2)-CO + $3C_2H_3$, and (2 × 2)-3CO on Rh(111). A mechanism for CO poisoning of ethylene hydrogenation on the metal single crystals was proposed, in which CO blocks surface metal sites and reduces adsorbate mobility to limit adsorption and reaction rate of ethylene and hydrogen.

1. Introduction

The nature of catalyst poisoning under reaction conditions is an important and unresolved question in catalysis science. Understanding the effects of coadsorbed species on the activity of catalysts is crucial in the development of more efficient catalysts. During reactions, the catalyst surface may be covered with undesirable adsorbates that may deactivate the catalyst, in addition to reactants, intermediates, and products. These adsorbates may render the catalytic surface inactive by blocking active surface sites or impeding the diffusion of adsorbed reactants and intermediates. Other adsorbates may promote the desired reactions by reducing activation energies or blocking undesired reaction pathways. For a reaction to occur the surface should remain flexible, atomic rearrangements should be possible, and adsorbate mobility should be high enough so that favorable adsorption sites can be accessed. Understanding the roles of coadsorbed species in catalytic reactions and their influence on catalytic surfaces at the high pressures employed in real catalysis is even more important, as the high incoming molecular flux at such conditions facilitates high adsorbate coverage, even above adsorbate desorption temperatures.

Scanning tunneling microscopy (STM) is a unique surface analysis probe that permits atomically resolved imaging of adsorbed species over a broad pressure range of $10^{-10}-10^{3}$ torr. High-pressure environments ensure that equilibrium between adsorbate structures and the gas phase is achieved. New and unexpected phenomena on catalytic surfaces have been previously reported at high pressures in comparison to what is observed under ultrahigh vacuum (UHV) conditions.[1−4] Furthermore, the ability of STM to image in situ with molecular details at high pressures makes STM a viable technique to monitor adsorbate mobility on the surface during catalytic reactions. This allows correlation between surface diffusion observed by STM and reaction rates as measured by methods such as mass spectrometry or gas chromatography.

In this paper we report on an STM study of ethylene hydrogenation and its poisoning by carbon monoxide on the Pt(111) and Rh(111) crystal surfaces. The reaction rates are high enough on both metal surfaces at room temperature to be detectable by mass spectrometry. We find that in the mtorr pressure range of both hydrogen and ethylene, the latter of which converts to mostly ethylidyne (C_2H_3) on the surfaces, the species adsorbed on the metal surfaces are very mobile. However, when CO is introduced into the system the catalytic reaction ceases abruptly and static ordered structures of the adsorbates are formed that can be readily imaged by STM. We interpret these results as due to the blocking of metal sites by CO, which prevents both the adsorption and mobility of ethylene and hydrogen on the surface necessary for the catalytic reaction. Poisoning occurs when surface mobility is suppressed and the adsorbate species become locked into static ordered structures.

2. Experimental Section

All experiments were carried out with a high-pressure, high-temperature STM system previously reported elsewhere.[5] The system consists of a UHV chamber containing surface preparation and analysis equipment, and an adjoining smaller chamber housing an STM (RHK Technology, Model VT-UHV 300) that allows experiments in UHV as well as at high pressures, with a working pressure and temperature ranges of $10^{-10}-10^{3}$ torr and 300−525 K. The base pressure of the system was 5×10^{-10} torr, with the background made up primarily of H_2, CO, and water.

Platinum and rhodium single-crystal samples of (111) orientation were used. The crystals were cut and polished to a miscut angle of less than 1°. Before each experiment the sample was prepared by sputtering with 400-eV oxygen ions for 10

* To whom correspondence should be addressed. Gabor A. Somorjai, Department of Chemistry, University of California, Berkeley, CA 94720. Tel: (510) 642-4053/Fax: (510) 643-9668. Email: somorjai@socrates.berkeley.edu.

[†] University of California, Berkeley.

[‡] Lawrence Berkeley National Laboratory.

10.1021/jp036580e CCC: $27.50
Published on Web 08/11/2004

min, followed by annealing in a vacuum at 1123 K for 10 min in the case of Pt(111) and 973 K for 2 min in the case of Rh(111). The sample cleanliness was checked with Auger electron spectroscopy. Just before the sample was transferred to the STM chamber, it was flashed to 1123 K for 2 min in the case of Pt(111) and 973 K for 1 min in the case of Rh(111).

During the experiments, the STM chamber was isolated from the rest of the system by gate valves. Hydrogen, ethylene, and carbon monoxide of ultrahigh purity grade were then introduced at room temperature in this order and allowed to equilibrate for 5 min before imaging under pressure after each addition. All STM images reported here were acquired using an electrochemically etched tungsten tip with the sample at room temperature and with settings of $I = 0.2$ nA and $V = 100$ mV. The STM chamber pressure during all experiments was monitored by a pressure transducer (MKS Instrument, Baratron 722A). The gas composition in the chamber was examined periodically by sampling gas through a leak valve to the mass spectrometer (Stanford Research Systems, RGA 200) in the UHV chamber.

3. Results

3.1. CO Poisoning of Ethylene Hydrogenation on Pt(111). Figures 1a and 1b show images of the platinum surface after addition of 20 mtorr each of hydrogen and ethylene. No ordered structures were detected, indicating rapid diffusion of the adsorbate species within the time scale of STM imaging (250 Å s^{-1}). The activity of the metal catalyst, and thus the presence of adsorbed reactants, was confirmed by ethane production detected by mass spectrometry. The hydrogenation rate was found to be 2.1×10^{-2} molecules $site^{-1}$ s^{-1} on Pt(111) at room temperature, lower than previously reported.[6] The lower measured reaction rate is due to the slow diffusion of the ethane product from the STM chamber to the UHV chamber through the sampling tubing. Upon the addition of CO, as low as 1 mtorr, to the hydrogen and ethylene mixture, production of ethane was no longer detected by mass spectrometry over the course of a week. The STM images revealed the presence of large domains of a hexagonal pattern rotated $22 \pm 1°$ with respect to the rhodium surface **(1 0)** vector, with a periodicity of 12.2 ± 0.3 Å and a corrugation of 0.3 ± 0.02 Å (Figure 1c). Figure 1d shows two hexagonal domains rotated by $7 \pm 1°$. No other ordered structures or disordered domains were observed on the surface.

3.2. CO Poisoning of Ethylene Hydrogenation on Rh(111). Similar to the Pt(111) case, no ordered structures could be detected by STM when the Rh(111) surface was exposed to 20 mtorr each of hydrogen and ethylene (Figures 2a and 2b). The ethylene hydrogenation rate under these conditions was found, by mass spectrometry, to be 1.3×10^{-4} molecules $site^{-1}$ s^{-1} at room temperature. Similar to the case of Pt(111), the measured reaction rate is believed to be lower than the actual rate, due to the slow diffusion rate of the product from the single crystal to the mass spectrometer as explained above. After the addition of 2 to 5.6 mtorr CO to gas phase, ethane production stopped as detected by mass spectrometry over the course of a week following the addition. STM images reveal the formation of several ordered structures, such as the c(4 × 2) structure shown in Figure 2c. Figure 3 shows a larger STM image showing several Rh(111) terraces separated by monatomic steps. They are covered by two visibly different domains. The brighter area, in the middle terrace in Figure 3, was found to be a mixture of c(4 × 2) and (4 × 2) structures. The darker areas consist of a (2 × 2) periodicity. Images of the c(4 × 2), (4 × 2), and (2 × 2) structures are shown in Figures 2c, 4a, and 4c, and the corresponding schematics of their proposed structures in Figures 2d, 4b, and 4d, respectively. Large domains of c(4 × 2) and (4 × 2) structures, rotated by 120°, could be observed with small

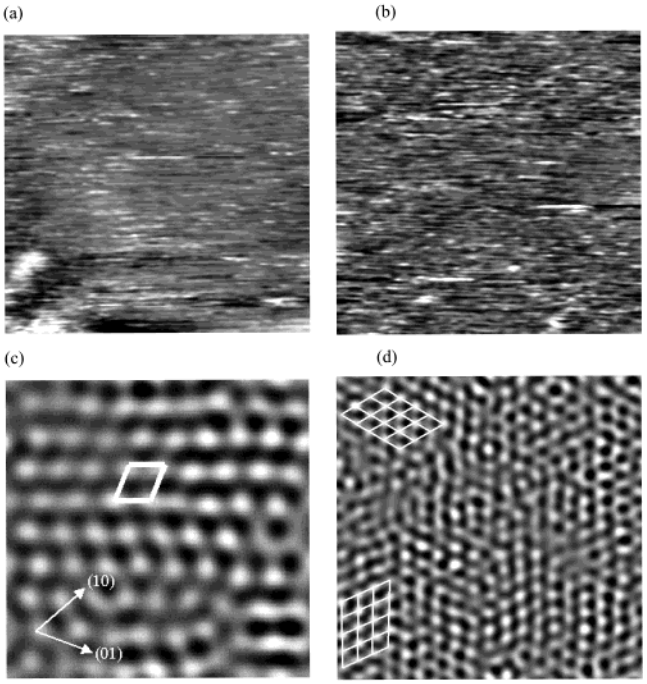

Figure 1. (100 × 100) Å^2 STM images of the Pt(111) surface under different pressures: (a) 20 mtorr H_2, (b) 20 mtorr H_2 and 20 mtorr ethylene, and (c) 20 mtorr H_2, 20 mtorr ethylene, and 2.5 mtorr CO. The presence of CO induced the formation of a $(\sqrt{19} \times \sqrt{19})$R23.4° structure on the surface. (d) (200 × 200) Å^2 STM image showing two rotational domains of $(\sqrt{19} \times \sqrt{19})$R23.4°.

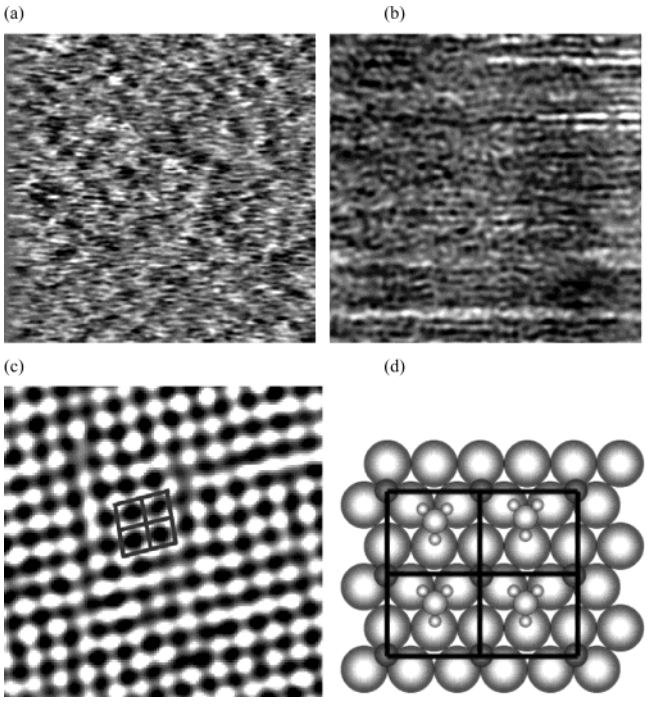

Figure 2. (100 × 100) Å^2 STM images of the Rh(111) surface under pressures of (a) 20 mtorr H_2 and (b) 20 mtorr H_2 and 20 mtorr ethylene. (c) (50 × 50) Å^2 STM image of c(4 × 2)-CO + C_2H_3 structure formed at 20 mtorr H_2, 20 mtorr ethylene, and 5.6 mtorr CO, and (d) a schematic showing the proposed structure of the corresponding unit cell as indicated in the image.

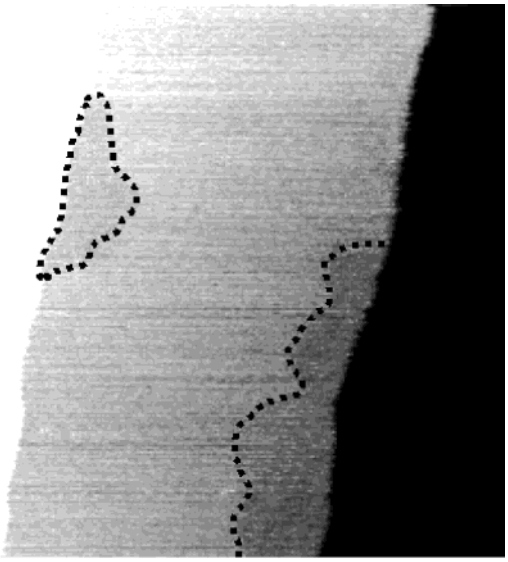

Figure 3. (1000 × 1000) Å^2 STM image of a Rh(111) terrace with two different regions at 20 mtorr H_2, 20 mtorr ethylene, and 5.6 mtorr CO. Images of the bright region shows that it is a combination of c(4 × 2) and (4 × 2) periodic structures. Those of the darker contrast (small outlined areas) show a (2 × 2) periodicity.

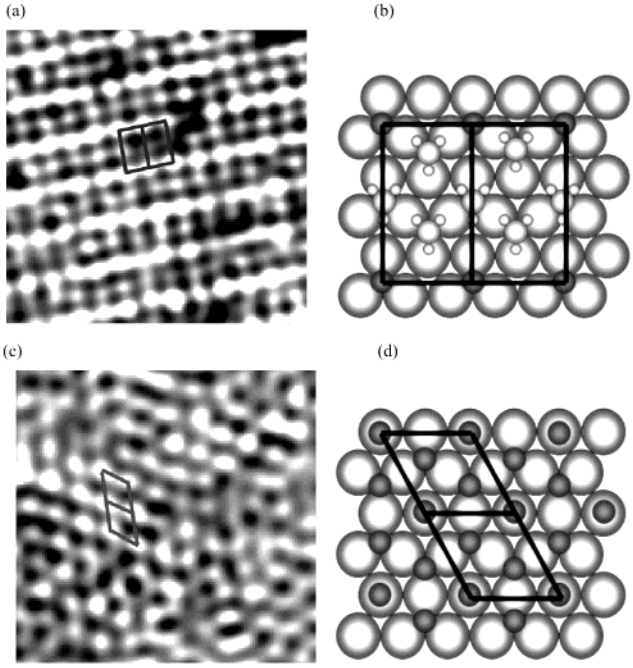

Figure 4. (50 × 50) Å^2 STM images of the (a) (4 × 2)-CO + $3C_2H_3$ and (b) (2 × 2)-3CO structures. Schematics (b) and (d) show the proposed structures of unit cells for the (4 × 2) and (2 × 2) structures, respectively.

(2 × 2) islands on the surface. Figure 5 shows domain boundaries between domains of (2 × 2), c(4 × 2), and (4 × 2). The c(4 × 2) structure has a corrugation of 0.21 ± 0.01 Å, and a rectangular periodicity of 4.3 ± 0.3 Å and 4.6 ± 0.2 Å. The (4 × 2) is similar to c(4 × 2) but with every other row having lower contrast, which doubles the unit cell size to a rectangular periodicity of 4.4 ± 0.3 Å and 8.9 ± 0.3 Å. The corrugation in the low contrast rows is 0.12 ± 0.02 Å, while in the higher contrast rows the corrugation is 0.19 ± 0.01 Å. The distance between each bright row and its adjacent dark row is 4.5 ± 0.3 Å. The (2 × 2) structural periodicity is 4.8 ± 0.4 Å, with a corrugation of 0.19 ± 0.03 Å.

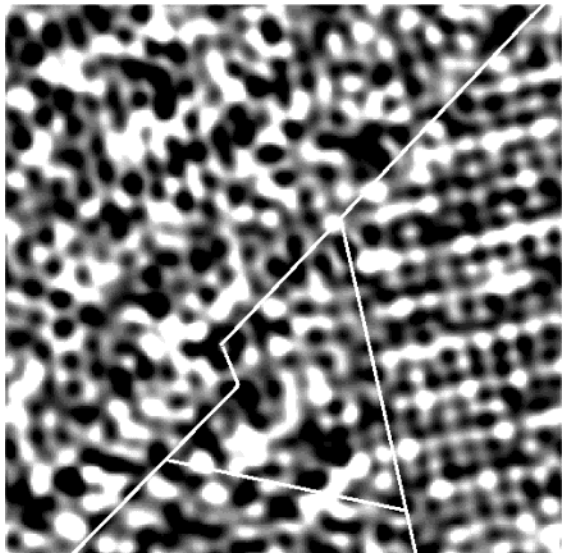

Figure 5. (100 × 100) Å^2 STM image of domain boundaries between (2 × 2), c(4 × 2), and (4 × 2) structures, from left to right, respectively.

4. Discussion

4.1. CO Poisoning of Ethylene Hydrogenation on Pt(111). The high surface mobility and small corrugation of hydrogen, 0.03 Å on platinum,[7,8] makes hydrogen difficult to image by STM at room temperature. It has been shown by electron energy loss spectroscopy,[9] helium diffraction,[7] and recoil scattering[8] experiments that hydrogen adsorbs dissociatively on platinum at threefold hollow sites, with face-centered cubic (fcc) hollow sites being slightly more energetically favorable and forming a (1 × 1) structure at saturation.[8,10,11]

The adsorption of ethylene on Pt(111) is well documented.[12−21] At temperatures below 50 K, ethylene is physisorbed with its C−C bond parallel to the surface.[12] Above 60 K it rehybridizes to form a di-σ-bonded state on fcc hollow sites.[13−16] The di-σ-bonded ethylene forms ethylidyne readily near room temperature through the loss of one hydrogen and transfer of another to the other carbon to form a methyl group.[22−24] At high pressure of ethylene or on surfaces precovered with hydrogen or ethylidyne, a second, more weakly adsorbed π-bonded ethylene has been shown to exist on top sites. This π-bonded species is believed to be directly involved in the catalytic hydrogenation process.[17,20] Ethylidyne is also rehydrogenated to ethylene, but only very slowly. Ethylidyne is essential in promoting the formation of the π-bonded, instead of the di-σ-bonded, ethylene on the surface;[6,23,25,26] the former can be readily hydrogenated to ethane, while steric hindrance makes hydrogen addition difficult to the latter.

High ethylidyne mobility, with a surface diffusion barrier smaller than 0.109 eV at high pressure,[27,28] explains the difficulty in observing this species with STM at room temperature. Ethylidyne has been shown by room-temperature low energy electron diffraction (LEED)[24,29] and low-temperature STM[21,29] to form a (2 × 2) structure (θ = 0.25 ML) on Pt(111) occupying fcc hollow sites, and reaching a nearly saturated coverage of 0.22 ML at room temperature.[30] At room temperature, however, ordered structures of ethylidyne could not be observed by STM, indicating rapid mobility on the time scale of STM imaging. Ethylidyne has been shown to be a spectator adsorbate during ethylene hydrogenation at high pressure,[6,23,25,26] even as it competes with H for the same adsorption sites. Thus, it appears that the high mobility of ethylidyne together with its open (2 × 2) structure, which allows hydrogen atoms to easily diffuse on

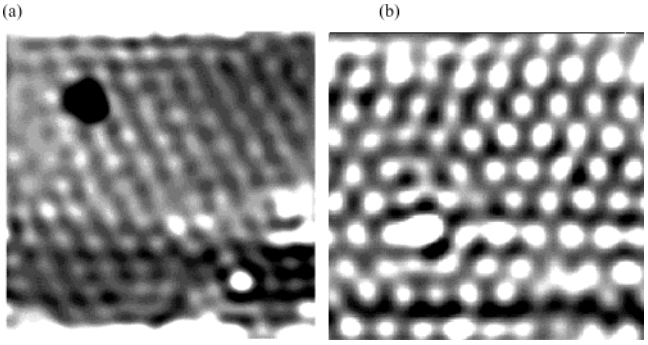

Figure 6. (100 × 100) Å^2 STM images of Pt(111) surface at (a) 5 mtorr CO and (b) 45 mtorr CO. The periodicity and corrugation is 11.4 ± 0.4 Å and 0.25 ± 0.04 Å in both cases, similar to the values found for the ($\sqrt{19} \times \sqrt{19}$)R23.4° structure formed by the coadsorption of hydrogen, ethylene, and CO at comparable pressure.

the surface and add to a weakly adsorbed π-bonded ethylene, is very important for the hydrogenation reaction to occur on a surface densely populated by adsorbates under high reaction pressure.

The (2 × 2) ethylidyne structure was observable by LEED, but not by STM, at room temperature due to the fact that in LEED the probing electron interacts with the surface on the time scale of picoseconds and therefore provides an "instantaneous" view of the structure. In contrast, in STM the interaction time between tip and surface is measured in milliseconds, and therefore cannot image molecules moving faster than such. The (100 × 100) Å^2 images obtained by STM in our current study were obtained at a scan rate of about 250 Å s^{-1}. This indicates that the surface diffusion rate of ethylidyne must be greater than this speed at room temperature, since no ethylidyne was imaged. In comparison to previous STM studies of ethylidyne performed under UHV,[21,29] the current study shows that neither a high background pressure of ethylene nor precovering the surface with hydrogen reduces the mobility of ethylidyne.

By adding CO to the Pt(111) surface precovered with hydrogen and ethylidyne, which has a diffusion activation energy of 0.130 eV at saturation coverage,[31] ordered structures could be resolved with STM indicating that the adsorbate mobility was notably decreased, whereas the rate of ethylene hydrogenation dropped to zero. The ordered structure formed is similar in corrugation and periodicity to the ($\sqrt{19} \times \sqrt{19}$)R23.4° ($\theta$ = 0.68 ML) structure previously examined under a higher pressure of pure CO.[32,33] Adsorption of pure CO on Pt(111) at similar pressures yielded the same hexagonal ordered pattern on the surface with comparable periodicity and corrugation (Figure 6). The images shown in Figure 1c and 1d show only one maximum per primitive unit cell. In the case of pure CO this maximum was assigned to an atop CO, due to its higher tunneling probability than that of CO at a threefold hollow site.[34]

Sum frequency generation (SFG)[35] and infrared spectroscopic[36] studies have shown that both CO and ethylidyne are present on the Pt(111) surface and that CO does not completely displace ethylidyne from the surface at room temperature during high-pressure coadsorption. The important question of whether ethylidyne and CO are mixed or segregated during coadsorption on Pt(111) is difficult to answer. On one hand, the observation of a ($\sqrt{19} \times \sqrt{19}$)R23.4° structure suggests pure domains of CO, with the ethylidyne segregating in regions between CO domains. Although we did not observe disordered patches or other domains that might indicate such segregation, this could be due to fast domain boundary mobility compared to the STM imaging time. The long-range order of the large ($\sqrt{19} \times \sqrt{19}$)R23.4°-13CO unit cell is a result of complex CO−CO and CO−substrate interactions extending to several neighbors; it is therefore unlikely to replace some of the CO molecules with ethylidyne while still maintaining the same large unit cell ordered structure.

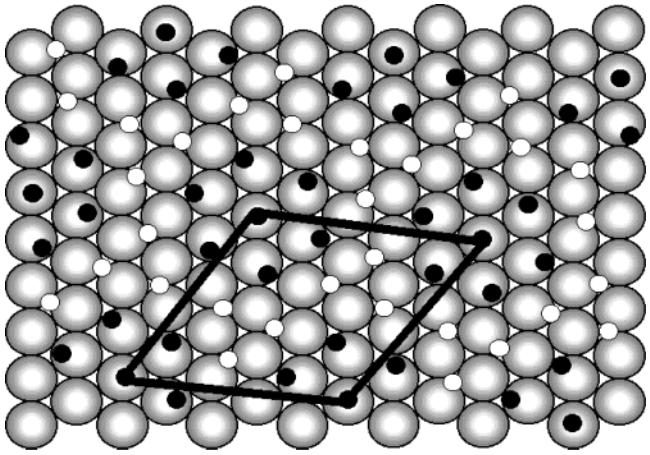

Figure 7. Model of ($\sqrt{19} \times \sqrt{19}$)R23.4° structure formed by the coadsorption of ethylene and CO. The gray, black, and white circles represent platinum atoms, atop and near-atop CO molecules, and possible ethylidyne replacements of CO at threefold hollow sites, respectively.

On the other hand, infrared spectroscopic studies have shown that high pressure coadsorption of ethylene and CO yields predominantly atop CO molecules and considerable interaction between CO and ethylidyne on Pt(111).[36] The red shift of atop CO stretch in infrared spectroscopy for CO on Pt(111) precovered with ethylidyne,[36] in comparison to CO on a clean Pt(111) surface, would indicate mixing of CO and ethylidyne on the surface. Since only large domains of ($\sqrt{19} \times \sqrt{19}$)R23.4° were visible on the surface with no evidence of disorder domains or other ordered structures, we cannot exclude that this observed ordered structure contains both CO and ethylidyne. Figure 7 shows a possible model for coadsorption of ethylene and CO within a ($\sqrt{19} \times \sqrt{19}$)R23.4° unit cell. This model has CO molecules occupy atop and near-atop sites and ethylidyne possibly replace CO molecules at threefold hollow sites, which could explain the infrared observation of mainly atop CO upon coadsorption. Since pure CO at comparable pressure forms the same incommensurate pattern on Pt(111) and the current STM used could not resolve molecules in the threefold hollow sites of the observed structure, we could not discern between ($\sqrt{19} \times \sqrt{19}$)R23.4° domains of pure CO and of mixed ethylidyne and CO structures on the surface. Assuming a complete replacement of CO by ethylidyne at the threefold hollow sites in the mixed unit cell, ethylidyne will have a coverage of 0.31 ML within the coadsorption domains. Thus, the coverage of ethylidyne changes from 0.22 ML initially on the surface before the addition of CO to a higher coverage of 0.31 ML within the coadsorption ($\sqrt{19} \times \sqrt{19}$)R23.4° structure. This means that both domains of pure CO and the mixed structure must be present on the surface. This agrees with previous SFG observations of two different atop CO stretches in the adsorption of CO on Pt(111) precovered with ethylidyne,[35] which represent two atop CO species with different neighboring adsorbates.

To see how CO affects the two key intermediates, π-bonded ethylene and adsorbed hydrogen, in the rate-determining step of ethylene hydrogenation on the catalytic Pt(111) surface, we can estimate the desorption rates and coverage of these two adsorbates under pressure in the presence of CO. The heat of

adsorption for CO at saturation coverage has been found by laser-induced thermal desorption to be 10 kcal/mol with a preexponential factor of $10^{7.5}$ s^{-1}.[37] By assuming the adsorption of π-bonded ethylene on a sterically hindered surface that is nearly saturated with ethylidyne and CO resembles physisorption,[21] we expect its heat of adsorption and preexponential factor to be on the order of 10 kcal/mol and 10^{12} s^{-1}.[38] This implies that the CO-to-ethylene ratio on the surface at high coverage in equilibrium with the gas phase is on the order of 10^4. Thus, we believe that most of the adsorbed π-bonded ethylene is replaced by CO due to the stronger binding of this species on the surface. In comparison, we anticipate any adsorbed hydrogen on the surface to remain on the surface after CO addition, and recombine and desorb slowly at room temperature, due to slow diffusion within the compact $(\sqrt{19} \times \sqrt{19})$R23.4° structure. We calculated the recombination and desorption rate of hydrogen within the less dense (2×2) ethylidyne structure to be 6.8×10^{-15} s^{-1} using the heat of adsorption and preexponential factor previously obtained by Zaera;[39,40] the rate should be even lower in the denser $(\sqrt{19} \times \sqrt{19})$R23.4° structure. The slow desorption rate of hydrogen, along with the lack of available π-bonded ethylene for hydrogen addition, means that hydrogen remains unreacted on the surface.

The CO poisoning of ethylene hydrogenation on Pt(111) is thus a result of the reduction in adsorbate mobility and of the blocking of surface metal sites. The immobile and dense ordered structures induced by CO impede mobility of ethylidyne and adsorbed hydrogen. They also block adsorption of additional reactants near these adsorbates. As a result of both decrease in adsorbate mobility and blocking of adsorption sites, the rate of ethylene hydrogenation drops to zero.

4.2. CO Poisoning of Ethylene Hydrogenation on Rh(111). Adsorptions of hydrogen[41,42] and ethylene[43−47] on Rh(111) have been determined to be quite similar to those on Pt(111) in past studies, with the noted difference of hydrogen[41] and ethylidyne[43] favoring hexagonal close-packed (hcp) hollow sites over fcc hollow sites on Rh(111) in forming (1×1) and (2×2) structures at room temperature, respectively. The conversion of ethylene to ethylidyne also occurs readily at a lower temperature of 170 K on Rh(111).[47] However, the current STM investigation on Rh(111) shows many similarities to the Pt(111) case and provides much insight into the poisoning effects of CO. During ethylene hydrogenation on Rh(111) at room temperature, atomic hydrogen, adsorbed ethylene, and ethylidyne were shown to be too mobile for STM to atomically resolve individual adsorbates.

The introduction of CO dramatically changed the situation, stopping the reaction completely as indicated by mass spectrometry. STM images of the poisoned surface showed ordered domains with large areas of $c(4 \times 2)$ and (4×2) periodicity and smaller regions of (2×2) periodicity. The formation of structures that could be imaged with molecular resolution is a consequence of the immobility of the adsorbed species in the STM time scale.

The $c(4 \times 2)$ ($\theta = 0.50$ ML) has been previously observed and studied by LEED after coadsorption of ethylene and CO, with a determined structure of CO occupying hcp hollow sites and ethylidyne fcc hollow sites.[48] A model is shown in the schematic of Figure 2d. The total coverage is 0.5 monolayer (ML). This structure does not form under the pressure of pure CO.[49] We propose that maxima at the corners of the rectangular unit cell observed by STM correspond to CO molecules, due to the similar corrugation of CO in rhodium threefold hollow sites previously reported.[49]

In this study a new (4×2) periodic structure ($\theta = 0.50$ ML) is also observed after coadsorption of ethylene and CO. This structure has a primitive unit cell twice as large as that of $c(4 \times 2)$, containing alternating rows of different contrasts. The species in the high contrast rows have the same corrugation and periodicity along the rows as those measured in the $c(4 \times 2)$. The dark rows also have similar periodicity but only nearly half the corrugation. The distance between two adjacent rows was measured to be a $\sqrt{3}$ multiple of rhodium−rhodium interatomic distance (2.69 Å), indicating that the observed molecules in both types of rows occupy the same type of adsorption sites. Thus, we conclude that the differently contrasted rows in the (4×2) structure were caused by two different molecules. H atoms are unlikely candidates, since in substrates where the structure has been imaged, they appear as depressions and their contrast is extremely small, on the order of 0.05 Å.[50,51] This leaves ethylidyne and CO as the only candidate molecules. Following the same argument as in the case of $c(4 \times 2)$, we assign the molecules in the bright rows to CO molecules and thus those in the dim rows to ethylidyne. Since CO molecules have similar corrugations at hcp and fcc hollow sites as previously found on Pd(111)[52] and we observed similar ordered structures in the absence of H_2, the two unobserved molecules inside the (4×2) primitive unit cell are assigned to be ethylidyne molecules occupying different sites from those in the dim rows. Thus, (4×2) appears as a unit cell with the less-conductive ethylidyne replacing CO molecules at every other row of the hcp hollow sites in the $c(4 \times 2)$. The proposed structure is shown in the schematic of Figure 4b.

Both the $c(4 \times 2)$ and (4×2) regions were observed on the surface in similar amounts, and intermixed in the form of patches. The mosaic distribution of $c(4 \times 2)$ and (4×2) structures of the same coverage density but different ethylidyne concentrations shows the formation is not thermodynamically equilibrated. This kinetically arrested configuration on the surface is most likely due to the low adsorbate mobility induced by CO coadsorption. Successive imaging of the same area over time did not show any exchange between different domains, indicating clearly low mobility of both ethylidyne and CO.

In addition to the above structures, small islands with (2×2) structure were observed along step edges on the surface, which we assign to be domains of (2×2)-3CO ($\theta = 0.75$ ML). Only the top site CO molecules were resolved by STM due to higher tunneling probability, similar to observations on other metals.[34,52] The corrugation and periodicity of the observed (2×2) agreed with that of the (2×2)-3CO formed on Rh(111) under high pressure of pure CO.[49] The observed order could not be caused by (2×2)-C_2H_3 since the open structure would allow adsorption of CO between ethylidyne, forming such mixed structures as $c(4 \times 2)$ and (4×2). In contrast, the denser (2×2)-3CO would be too compact for ethylene to adsorb. The lack of agreement of the observed (2×2) corrugation with that of ethylidyne as examined in (4×2) further confirms that the observed structure was (2×2)-3CO and not immobilized (2×2)-C_2H_3 islands.

Imaging across the rhodium surface revealed no disordered areas. The bright regions of the $c(4 \times 2)$-CO+C_2H_3 and (4×2)-CO+$3C_2H_3$ domains were observed to cover 77.2% of the surface, with the remaining occupied by the (2×2)-3CO structures in the darker areas. Within the observed bright areas, 48.8% of the surface was of $c(4 \times 2)$ and 51.2% (4×2). Assuming CO coadsorption has no effects on either ethylidyne formation or rehydrogenation (and thus desorption), and using the proposed structures for the observed orders above, the initial

coverage of ethylidyne on the Rh(111) surface prior to the CO addition is thus calculated to be 0.242 ML. Given that ethylidyne molecules organize into a (2×2) order on a Rh(111) surface at room temperature, this indicates the initial Rh(111) surface prior to poisoning under the current hydrogenation condition is already covered with this inert spectator species and nearly saturated by the (2×2)-C_2H_3 structures.

The formation of ordered structures and the drastic decrease in reaction rate upon the addition of CO show the similarities of the poisoning mechanism by CO on ethylene hydrogenation on Pt(111) and Rh(111). The presence of $c(4 \times 2)$ and (4×2) on Rh(111) confirms that the introduction of CO does not completely displace ethylidyne from the surface, but reduces surface mobility by confining surface species such as ethylidyne within nonmobile CO-induced structures. This is much in contrast to the (2×2)-C_2H_3 structures of the active surface formed in the absence of CO that allow adsorbates to be mobile. No reaction occurs on the poisoned surface of $c(4 \times 2)$ and (4×2) periodicity, even though the concentration of ethylidyne in these structures is comparable to the unpoisoned (2×2)-C_2H_3 surface. Due to the reduced mobility induced by CO, ethylidyne becomes a poison to the metal catalyst surface. The regions of (2×2)-3CO structure show no catalytic activity toward ethylene hydrogenation, due to the high density coverage of immobile adsorbates excluding additional adsorption in those areas. As with the case of Pt(111), we propose that CO replaces weakly adsorbed ethylene and blocks ethylidyne mobility, reducing available surface metal sites for additional adsorption of hydrogen and ethylene and leading to slower diffusion of adsorbed hydrogen and ethylene across the Rh(111) surface, thus causing a termination of ethylene hydrogenation.

5. Conclusions

The poisoning effects of CO on ethylene hydrogenation were studied by STM on Pt(111) and Rh(111) single-crystal surfaces in the mtorr range at room temperature. The rates of ethylene hydrogenation on both metal surfaces were shown to drop to zero upon the addition of CO. While adsorbed hydrogen, ethylene, and ethylidyne were too mobile to be observable by STM on Pt(111) and Rh(111) surfaces, the presence of CO reduced adsorbate mobility and induced static ordered structures on the surfaces that could be imaged by STM. A $(\sqrt{19} \times \sqrt{19})$R23.4° structure was found for the coadsorption of ethylene and CO that is similar to that observed at the same pressure of pure CO. The addition of CO to the Rh(111) surface precovered with hydrogen and ethylene resulted in three different ordered patterns on the surface. A $c(4 \times 2)$-CO + C_2H_3 structure was observed, along with a new, previously unobserved (4×2)-CO + $3C_2H_3$ structure. We conclude that alternating rows of this new (4×2) structure are the result of replacement of CO by ethylidyne. A (2×2)-3CO structure was also observed on the Rh(111) surface, indicating that regions with pure CO are also formed, as in the case of Pt(111).

The present results clearly indicate that mobility of the surface species is an essential condition for catalytic action on the densely covered catalyst surfaces. The importance of adsorbate mobility for adsorption has recently been shown in the case of H_2 dissociation on Pd(111), where near-saturation-coverage thermally activated statistical fluctuations were found to be necessary to bring together three or more vacancies needed for the molecule to dissociate.[51] At lower temperature, when H became immobile, no aggregation of vacancies occurred and H_2 dissociative chemisorption stopped. Here we show that adsorbate mobility is necessary not only for adsorption of the reactants but also for the reaction between adsorbates to occur. We have shown that the presence of the site-blocking, but mobile, ethylidyne does not poison the ethylene hydrogenation reaction, even if ethylidyne occupies the same sites as H. Mobility facilitates statistical fluctuations in surface adsorbate density that open up sites for both gas-phase molecules to adsorb and dissociate, as well as for adsorbed species to diffuse across the surface and react. When ethylidyne is immobilized by CO coadsorption, ethylidyne becomes a poison to the catalyst and the reaction stops. The STM results indicate that the poisoning mechanism of CO on ethylene hydrogenation on Pt(111) and Rh(111) are similar, with CO lowering adsorbate mobility and inducing static ordered structure on both surfaces. This, in turn, prevents the statistical fluctuation necessary for availability of surface metal sites for reactant adsorption under high pressures. We propose that CO replaces most of the weakly adsorbed π-bonded ethylene and prevents further adsorption, while the dense CO-induced ordered structure immobilizes and traps atomic hydrogen on the surface, thus preventing ethylene hydrogenation. This poisoning mechanism of CO entails that any adsorbate that has a long resident time and lowers surface mobility can become an effective poisoning reagent to a catalytic surface.

In both cases of ethylene hydrogenation on Pt(111) and Rh(111), we found that adsorbate mobility was a crucial factor. These observations extend our understanding of the mechanisms of catalysis by demonstrating that the presence of inert spectators and poison species is only a part of the catalytic process. In addition, adsorbate mobility and modifiers of this mobility are also essential factors that need to be understood as well.

Acknowledgment. This work was supported by the Director, Office of Science, Office of Basic Energy Sciences, Division of Materials Science and Engineering, of the U.S. Department of Energy under Contract No. DE-AC03-76SF00098.

References and Notes

(1) McIntyre, B. J.; Salmeron, M.; Somorjai, G. A. *J. Vac. Sci. Technol. A* **1993**, *11*, 1964.
(2) Su, X.; Cremer, P. S.; Shen, Y. R.; Somorjai, G. A. *Phys. Rev. Lett.* **1996**, *77*, 3858.
(3) Hendriksen, B. L. M.; Frenken, J. W. M. *Phys. Rev. Lett.* **2002**, *89*, 46101.
(4) Thostrup, P.; Kruse Vestergaard, E.; An, T.; Lægsgaard, E.; Besenbacher, F. *J. Chem. Phys.* **2003**, *118*, 3724.
(5) Jensen, J. A.; Rider, K. B.; Chen, Y.; Salmeron, M.; Somorjai, G. A. *J. Vac. Sci. Technol. B* **1999**, *17*, 1080−1084.
(6) Zaera, F.; Somorjai, G. A. *J. Am. Chem. Soc.* **1984**, *106*, 2288.
(7) Lee, J.; Cowin, J. P.; Wharton, L. *Surf. Sci.* **1983**, *130*, 1.
(8) Umezawa, K.; Ito, T.; Asada, M.; Nakanishi, S.; Ding, P.; Lanford, W. A.; Hjorvarsson, B. *Surf. Sci.* **1997**, *387*, 320.
(9) Baro, A. M.; Ibach, H.; Bruchmann, H. D. *Surf. Sci.* **1979**, *88*, 384.
(10) Batra, I. P.; Barker, J. A.; Auerbach, D. J. *J. Vac. Sci. Technol. A* **1984**, *2*, 943.
(11) Christmann, K. *Surf. Sci. Rep.* **1988**, *9*, 1.
(12) Cassuto, A.; Kiss, J.; White, J. M. *Surf. Sci.* **1991**, *255*, 289.
(13) Steininger, H.; Ibach, H.; Lehwald, S. *Surf Sci.* **1982**, *117*, 685.
(14) Doll, R.; Gerken, C. A.; Van Hove, M. A.; Somorjai, G. A. *Surf. Sci.* **1997**, *374*, 151.
(15) Cremer, P.; Stanners, C.; Niemantsverdriet, J. W.; Shen, Y. R.; Somorjai, G. *Surf. Sci.* **1995**, *328*, 111.
(16) Ibach, H.; Lehwald, S. *J. Vac. Sci. Technol.* **1978**, *15*, 407.
(17) Cremer, P. S.; Su, X. C.; Shen, Y. R.; Somorjai, G. A. *J. Am. Chem. Soc.* **1996**, *118*, 2942.
(18) Carlsson, A. F.; Madix, R. J. *J. Chem. Phys.* **2001**, *115*, 8074.
(19) Watson, G. J.; Wells, R. P. K.; Willock, D. J.; Hutchings, G. J. *J. Phys Chem. B* **2000**, *104*, 6439.
(20) Ofner, H.; Zaera, F. *J. Am. Chem. Soc.* **2002**, *124*, 10982.
(21) Land T. A.; Michely T.; Behm R. J.; Hemminger J. C.; Comsa G. *Appl. Phys. A* **1991**, *53*, 414.
(22) Cremer, P. S.; Somorjai, G. A. *J. Chem. Soc., Faraday Trans.* **1995**, *91*, 3671.

(23) Zaera, F.; French, C. R. *J. Am. Chem. Soc.* **1999**, *121*, 2236.
(24) Starke, U.; Barbieri, A.; Materer, N.; Van Hove, M. A.; Somorjai, G. A. *Surf. Sci.* **1993**, *286*, 1.
(25) Ofner, H.; Zaera, F. *J. Phys. Chem. B* **1997**, *101*, 396.
(26) Zaera, F. *Langmuir* **1996**, *12*, 88.
(27) Nomikou, Z.; Van Hove, M. A.; Somorjai, G. A. *Langmuir* **1996**, *12*, 1251.
(28) The calculated value from Land et al.[21] was based on single molecular diffusion. We believe the diffusion barrier to be much lower at near-saturation due to ethylidyne−ethylidyne repulsive interaction and weaker binding to the surface due to electron donation to the surface from more ethylidyne molecules.
(29) Land, T. A.; Michely, T.; Behm, R. J.; Hemminger, J. C.; Comsa, G. *J. Chem. Phys.* **1992**, *97*, 6774.
(30) Abon, M.; Billy, J.; Bertolini, J. C. *Surf. Sci.* **1986**, *171*, L387.
(31) Ma, J.; Xiao, X.; DiNardo, N. J.; Loy, M. M. T. *Phys. Rev. B* **1998**, *58*, 4977.
(32) Kruse Vestergaard, E.; Thostrup, P.; An, T.; Lægsgaard, E.; Stensgaard, I.; Hammer, B.; Besenbacher, F. *Phys Rev. Lett.* **2002**, *88*, 259601.
(33) Another high-pressure CO structure has also been proposed but subsequently refuted by Kruse Vestergaard et al.[32] Jensen, J. A.; Rider, K. B.; Salmeron, M.; Somorjai, G. A. *Phys. Rev. Lett.* **1998**, *80*, 1228.
(34) Chiang, S.; Wilson, R. J.; Mate, C. M.; Ohtani, H. *Vacuum* **1990**, *41*, 118.
(35) Chen, P.; Kung, K. Y.; Shen, Y. R.; Somorjai, G. A. *Surf. Sci.* **2001**, *494*, 289.
(36) Ainsworth, M. K.; McCoustra, M. R. S.; Chesters, M. A.; Sheppard, N.; De La Cruz, C. *Surf. Sci.* **1999**, *437*, 9.
(37) Seebauer, E. G.; Kong, A. C. F.; Schmidt, L. D. *Surf. Sci.* **1986**, *176*, 134.
(38) The physisorption of π-bonded ethylene was assumed to resemble that of noble gases on Pt(111). The preexponential factor and heat of adsorption of the latter have been previously investigated by Widdra, W.; Trischberger, P.; Friess, W.; Menzel, D.; Payne S. H.; Kreuzer, H. J. *Phys. Rev. B* **1998**, *57*, 4111.
(39) Zaera, F. *J. Phys. Chem.* **1990**, *94*, 8350.
(40) The "abnormally low" preexponential value for hydrogen desorption has been previously explained by (a) Poelsema, B.; Mechtersheimer, G.; Comsa, G. *Surf. Sci.* **1981**, *111*, 519 and (b) Poelsema, B.; Mechtersheimer, G.; Comsa, G. *Surf. Sci.* **1981**, *111*, L728.
(41) Payne, S. H.; Kreuzer, H. J.; Frie, W.; Hammer, L.; Heinz, K. *Surf. Sci.* **1999**, *421*, 279.
(42) Yanagita, H.; Fujioka, H.; Aruga, T.; Takagi, N.; Nishijima, M. *Surf. Sci.* **1999**, *441*, 507.
(43) Wander, A.; Van Hove, M. A.; Somorjai, G. A. *Phys Rev. Lett.* **1991**, *67*, 626.
(44) Bowker, M.; Gland, J. L.; Joyner, R. W.; Li, Y.; Slin'ko, M. M.; Whyman, R. *Catal. Lett.* **1994**, *25*, 293.
(45) Bent, B. E.; Mate, C. M.; Kao, C. T.; Slavin, A. J.; Somorjai, G. A. *J. Phys. Chem.* **1988**, *92*, 4720.
(46) Calhorda, M. J.; Lopes, P. E. M.; Friend, C. M. *J. Mol. Catal. A* **1995**, *97*, 157.
(47) Papageorgopoulos, D. C.; Ge, Q.; King, D. A. *Surf. Sci.* **1998**, *397*, 13.
(48) Blackman, G. S.; Kao, C. T.; Bent, B. E.; Mate, C. M.; Van Hove, M. A.; Somorjai, G. A. *Surf. Sci.* **1988**, *207*, 66.
(49) Cernota, P.; Rider, K.; Yoon, H. A.; Salmeron, M.; Somorjai, G. *Surf. Sci.* **2000**, *445*, 249.
(50) Lauhon, L. J.; Ho, W. *Phys. Rev. Lett.* **2000**, *85*, 4566.
(51) Mitsui, T.; Rose, M. K.; Fomin, E.; Ogletree, D. F.; Salmeron, M. *Nature* **2003**, *422*, 705.
(52) Rose, M. K.; Mitsui, T.; Dunphy, J.; Borg, A.; Ogletree, D. F.; Salmeron, M.; Sautet, P. *Surf. Sci.* **2002**, *512*, 48.